Charge conveyance and nonlinear acoustoelectric phenomena for intense surface acoustic waves on a semiconductor quantum well

M. Rotter, A. V. Kalameitsev, A. O. Govorov, W. Ruile, Achim Wixforth

Angaben zur Veröffentlichung / Publication details:

Rotter, M., A. V. Kalameitsev, A. O. Govorov, W. Ruile, and Achim Wixforth. 1999. "Charge conveyance and nonlinear acoustoelectric phenomena for intense surface acoustic waves on a semiconductor quantum well." *Physical Review Letters* 82 (10): 2171–74. https://doi.org/10.1103/physrevlett.82.2171.

Charge Conveyance and Nonlinear Acoustoelectric Phenomena for Intense Surface Acoustic Waves on a Semiconductor Quantum Well

M. Rotter,[1] A. V. Kalameitsev,[2] A. O. Govorov,[2] W. Ruile,[3] and A. Wixforth[1]
[1]*Sektion Physik der LMU and CeNS, Geschwister-Scholl-Platz 1, 80539 München, Germany*
[2]*Institute of Semiconductor Physics, 630090 Novosibirsk, Russia*
[3]*Siemens AG, Corporate Technology, 81730 München, Germany*
(Received 7 December 1998)

The combination of semiconductor quantum well structures and strongly piezoelectric crystals leads to a system in which surface acoustic waves with very large amplitudes can interact with charge carriers in the well. The surface acoustic wave induces a dynamic lateral superlattice potential in the plane of the quantum well which is strong enough to spatially break up a two-dimensional electron system into moving wires of trapped charge. This transition is manifested in an increase of the electron transport velocity with sound amplitude, eventually reaching the sound velocity. The sound absorption by the electron system then becomes governed by nonlinearities and is strongly reduced. We study the transition from the linear towards the strongly nonlinear regime of interaction and present a theoretical description of such phenomena in a 2D system. [S0031-9007(99)08621-4]

PACS numbers: 73.50.Rb, 72.50.+b, 73.50.Fq

Electron transport in semiconductor quantum well structures is usually governed by drift or diffusive current flow. Also ballistic carrier motion can be observed, provided that the size of the system is smaller than the mean-free path, ranging up to some hundred microns in very pure semiconductor material. Conceptually different from those mechanisms are transport phenomena based on momentum transfer from externally propagating entities to the electron system. Such "dragging" experiments have been studied in great detail in double electron layer systems [1], where internal "Coulomb friction" between the two layers causes the dragging force. "Photon drag" induced transport was observed for intersubband transitions of a quasi-two-dimensional electron system (2DES) [2]. Nagamune *et al.* [3] observed the effect of a dc current on the drift of optically generated carriers in a quantum well. Acoustic charge transport (ACT) has been investigated on a variety of different systems in view of possible device applications [4]. Using surface acoustic waves (SAW), Rocke *et al.* [5] showed that photogenerated electron-hole pairs in a semiconductor quantum well can be efficiently trapped in the moving lateral potential of the sound wave and then be reassembled into photonic signals. Recently, SAW have been combined with Coulomb blockade to drive single electrons through a quantum point contact [6]. In addition, the interaction between SAW and mobile charges in semiconductor layered structures has become an important method to study the dynamic conductivity of low-dimensional systems in quantum wells. These studies include the integer quantum Hall effect [7], the fractional quantum Hall effect [8], Fermi surfaces of composite Fermions around a half-filled Landau level [9], and commensurability effects caused by the lateral superlattice induced by a SAW [10]. These studies, however, were restricted to the small signal limit, i.e., to a regime where the presence of the lateral potential of a piezoelectric wave does not significantly modulate the carrier density in the quantum well.

Here, we would like to report on experiments, where we employ SAW with a large piezoelectric potential amplitude comparable to the band gap of the semiconductor. Such high SAW potentials strongly modulate the equilibrium density distribution of the electron system in a quantum well. This leads to a new and nonlinear interaction between the wave and the carriers, eventually breaking up the electron system into spatially separated wires of charge. These wires are propagating at the speed of sound in the direction of the wave. It is very difficult to realize SAW with such large amplitudes on GaAs-based structures. Therefore, we introduced a hybridization technique, where we use the strong piezoelectricity of a host crystal ($LiNbO_3$) to couple the fields of a SAW to the electron system in GaAs-based quantum wells [11]. We fabricate these hybrid structures employing an epitaxial lift-off (ELO) technique [12]. The semiconductor layered system is grown by molecular beam epitaxy, starting with an AlAs sacrificial layer above the GaAs substrate. This layer is followed by the active heterostructure containing an $In_{0.2}Ga_{0.8}As$ quantum well embedded in modulation doped $Al_{0.2}Ga_{0.8}As$ barriers. The 12 nm InGaAs quantum well contains a high quality 2DES ($\mu > 5000\ cm^2/V\,s$ at room temperature), to which Ohmic contacts are formed. By etching the AlAs layer, we remove the active semiconductor layer from the substrate and transfer it to the $LiNbO_3$ [11]. There, the film is tightly bonded to the substrate surface by van der Waals forces. Metal interdigital transducers (IDT) on the $LiNbO_3$ serve to launch and detect the SAW. Then the ELO film is patterned and provided with a thin NiCr film acting as a gate electrode. The distance between the 2DES and the $LiNbO_3$ surface is just 32 nm, whereas the distance

between the 2DES and the gate electrode is 450 nm in order to reduce the screening of the SAW fields by the electrode. To examine the transport properties of the electron system in the traveling acoustic wave, we developed the sample geometry shown in Fig. 1. A continuous rf signal is applied to the left IDT and generates a continuous SAW. The center part of the ELO film represents the transport region, where electrons are traveling in the wave potential. A corresponding transport gate is used to control the electron density N_s (Fig. 1). For optimum transport conditions, a negative transport voltage $V_t = -8$ V is applied to this gate, such that the electron system is nearly depleted. To charge the traveling wave potential wells with electrons, a narrow injection gate is used, as indicated in Fig. 1. Removing the otherwise negative bias at this gate for a short moment (0.3 μs) injects charge into the potential wells of the SAW. The traveling lateral potential wells of the SAW flush a certain amount of these electrons into the transport region, where they can be completely trapped in the valleys of the SAW potential. When leaving the transport channel, they are swept into the region of a third gate, acting as a Schottky diode charge detector, which can be read out with an oscilloscope.

Figure 2 shows this detected transport signal as a function of time and SAW intensity at room temperature. In this case the frequency is $f = 340$ MHz, corresponding to a SAW wavelength of about $\lambda = 10$ μm. The lowest trace displays the voltage applied to the injection gate (right vertical axis) showing that electrons are injected for $\Delta t = 335$ ns. The upper family of traces represents the detected charge signal for different SAW intensities, where the lowest trace corresponds to the highest rf power (30.5 dBm, corresponding to 72 W/m). At this high power, a large signal is detected at the read-out gate after a delay time of 650 ns. Remarkably, with decreasing SAW amplitude, the detected signal broadens and the time delay between injection and detection increases significantly.

In order to understand these phenomena we developed a nonlinear theory for the acoustoelectric interaction in 2D [13]. Most of the former theoretical studies [14] on the SAW absorption and the drag in 2D electron systems relate to the linear regime of the interaction, when the equilibrium electron density N_s is much larger than the perturbation $\delta n_s(x,t)$ caused by the SAW. Here t and x are the time and the in-plane coordinate along the SAW-propagation direction, respectively. However, in our system, the SAW amplitude is so large that we have to consider nonlinear phenomena. In a simple approach, the surface electron current is well described by the Drude model, $j(x,t) = \sigma(x,t)E_x(x,t)$, where $\sigma(x,t) = e\mu n_s(x,t)$ is the sheet conductivity, μ is the mobility, $n_s(x,t)$ is the modulated electron density, and E_x is the in-plane electric field. To make the problem self-consistent we write $E_x = E_{\mathrm{SAW}} + E_{\mathrm{ind}}$, where E_{SAW} and E_{ind} are created by the SAW and the perturbed electron density $n_s(x,t)$, respectively. The electric field of the SAW has the usual form $E_{\mathrm{SAW}} = E_0 \sin(kx - \omega t)$, where k denotes the SAW wave vector. Then, the potential induced by the electron plasma ϕ_{ind} is determined by the function $n_s(x,t)$. The

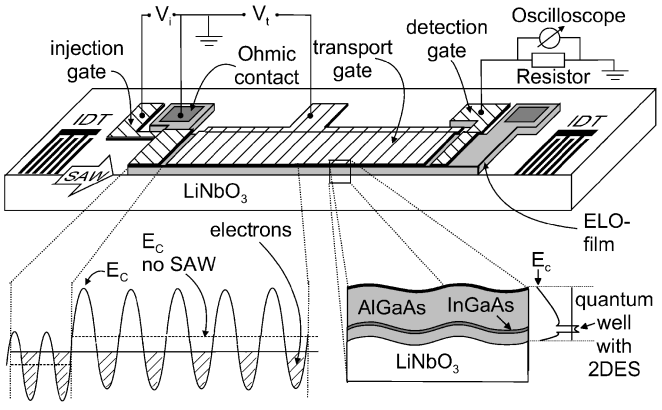

FIG. 1. Schematic sketch of a cut through the symmetry axis along the SAW propagation direction of the sample. The thin GaAs film (not drawn to scale) is partially covered by gate electrodes. Also shown is a schematic picture of the conduction band E_C being modulated by the SAW potential at the time of charge injection. The vertical layer system, including the vertical conduction band structure, is also displayed.

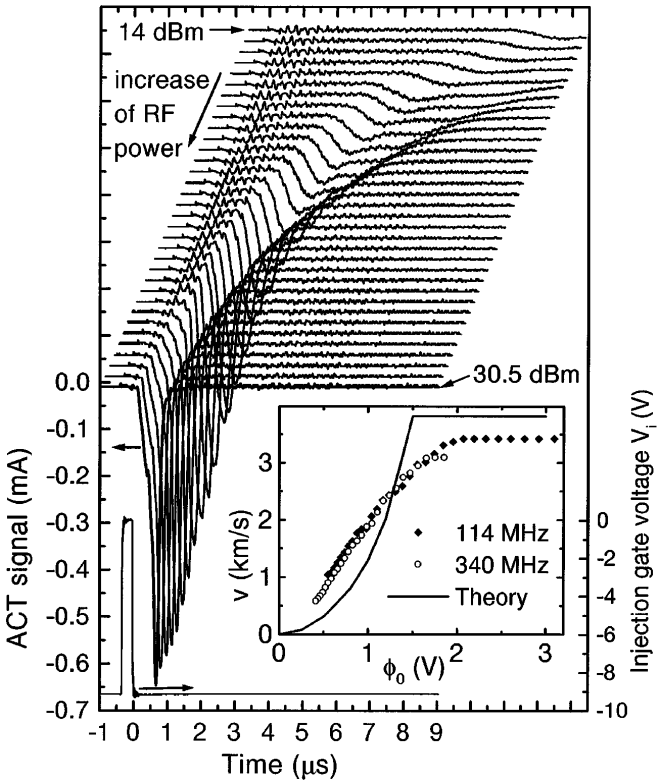

FIG. 2. Injection gate voltage and signal at the detection gate as a function of time at room temperature. Between each trace of the ACT signal, the applied power was changed by 0.5 dB. For clarity, the curves are shifted against each other. The inset shows the measured transport velocity as a function of SAW power and the calculated velocity.

Fourier transforms of these quantities are connected via $\phi_{\rm ind}(q,t) = -en_s(q,t)/[\epsilon_{\rm eff}(|q|)|q|]$ [15], where the effective dielectric constant $\epsilon_{\rm eff}(|q|) = \epsilon_0(\epsilon_p + \epsilon_s \coth|q|a)$, and ϵ_p and ϵ_s are the dielectric constants of the piezoelectric and semiconductor crystals, respectively. a is the distance between the 2DES and the gate. $n_s(x,t)$ is described by the continuity equation $e\partial n_s/\partial t - \partial j/\partial x = 0$. All quantities in our equations depend only on $(x - vt)$, where v denotes the SAW velocity. Thus we can introduce a new variable $x_1 = x - vt$. The resulting equation for $n_s(x_1)$ turns out to be both nonlinear and nonlocal. In a gated system, such as in our case, we can simplify this equation in the long wavelength limit $ka \ll 1$ [16]. In this limit the connection between $\phi_{\rm ind}$ and n_s becomes local, $\phi_{\rm ind}(x_1) = -ean_s(x_1)/(\epsilon_0\epsilon_s)$. Then, after one integration in the continuity equation, we get

$$en_s\mu\left[\frac{ea}{\epsilon_0\epsilon_s}\frac{dn_s}{dx_1} + E_0\sin(kx_1)\right] + evn_s = A_0\,, \quad (1)$$

where A_0 is a constant. The solution of Eq. (1) should be periodic and continuous. Numerical solutions for various average 2D densities $N_s = \langle n_e(x_1)\rangle$ are shown in the inset of Fig. 3. Here the brackets $\langle\cdots\rangle$ denote the average over λ. It can be seen that the electron system forms separated stripes for small values of N_s. $\Phi_0 = E_0/k$ is the amplitude of the SAW potential. It follows from Eq. (1) that in the regime of separated strips $A_0 = 0$, and the average local velocity of the electron plasma, $\langle v_e(x_1)\rangle = \langle j\rangle/eN_s$, is at its maximum and equal to the sound velocity v.

In the inset of Fig. 2 we plot the experimental data for the average velocity of the conveyed electrons as calculated from the length of the transport channel (2 mm) and the delay time of the maximum of the charge signal. With increasing SAW intensity, this velocity also increases and eventually saturates at the SAW velocity. Two sets of data taken at $f = 340$ MHz and $f = 114$ MHz are shown. The potential Φ_0 is calculated from the SAW intensity $I_{\rm SAW}$. Also depicted in the inset is the result of our numerical calculation of the average velocity using the parameters $N_s = 2.5 \times 10^{10}$ cm^{-2} and $\mu = 5000$ cm^2/V s. Our relatively simple model reproduces the experimental behavior very well. The saturation of v_e reflects the formation of electron stripes.

The SAW piezoelectric fields can be so strong that a bunching of charge can occur in a formerly homogeneous electron system in the well. For this reason, we investigate the SAW transmission through a homogeneous electron system as a function of SAW power. As has been shown before [14] in the small signal limit, the attenuation of the SAW depends on the sheet conductivity of the 2DES, exhibiting a maximum at a certain conductivity σ_m. For large SAW intensities, however, the attenuation Γ behaves quite differently: Γ is strongly reduced

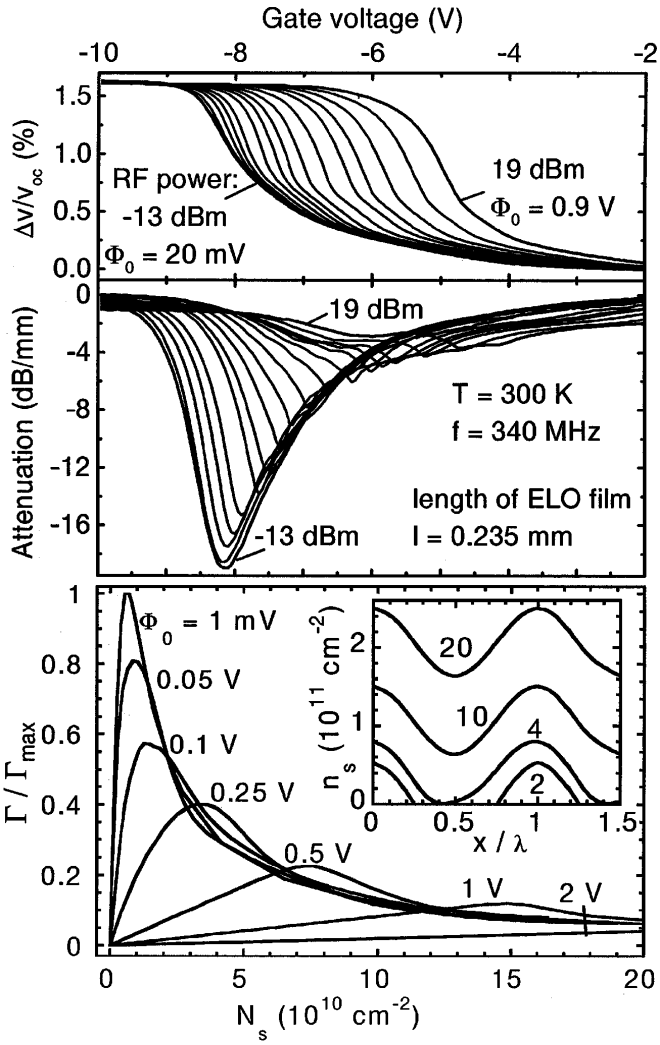

FIG. 3. Measured attenuation and velocity change of a SAW as a function of gate voltage for different rf power. The lower part shows the calculated attenuation as a function of the carrier concentration N_s. In the inset we plot the calculated local carrier concentration n_s as a function of the in-plane coordinate for different total carrier concentration N_s. The numbers attached to the plots correspond to N_s in units of 10^{10} cm^{-2}.

with increasing SAW power and the maximum attenuation shifts to smaller gate bias and thus higher conductivity. This experimental finding is shown in Fig. 3, where we plot the electronic SAW attenuation as a function of gate bias and for different SAW power levels. In this case, the sample is a hybrid in which a single homogeneous gate electrode is used to change the carrier concentration underneath.

The absorption of the SAW by the electrons is given by the quantity $Q = \langle jE_{\rm SAW}\rangle$. When the electron velocity v_e becomes equal to v, the SAW absorption Q also reaches its maximum, $Q_{\rm max} = ev^2N_s/\mu$. This can also be seen from the following: In the Drude model, the absorption can be written as $Q = \langle jE_{\rm SAW}\rangle = \langle m^*n_s(x)v_e^2(x)/\tau\rangle$, where m^* and τ are the effective electron mass and the relaxation

time, respectively. When $v_e(x)$ becomes equal to v, the dissipation reaches its maximum, $Q = Q_{\max}$. The nonlinear absorption coefficient, $\Gamma = Q/I_{\mathrm{SAW}}$, as a function of N_s was calculated using the solutions of Eq. (1) (see the lower part of Fig. 3). For small intensities, Γ is given by the well-known formula [14],

$$\Gamma_0 = \frac{K_H^2}{2} k \frac{\sigma/\sigma_m}{1 + (\sigma/\sigma_m)^2}, \qquad (2)$$

where $\sigma_m = \epsilon_{\mathrm{eff}} v$ and K_H^2 is the effective electromechanical coupling coefficient of the layered system [17]. In our system, K_H^2 is 2 orders of magnitude larger than on monolithic GaAs. In the limit of high Φ_0 the absorption coefficient is given by $\Gamma = Q_{\max}/I_{\mathrm{SAW}} \propto 1/I_{\mathrm{SAW}}$ and decreases with increasing SAW intensity. Theory and experiment are in good agreement: For large SAW power, the calculated absorption coefficient decreases and the position of the maximum of the attenuation is shifted towards higher carrier concentration.

The shift of the SAW velocity due to the electron plasma in a linear theory [14] is given by $2(v - v_{sc})/v_{oc} = K_H^2/[1 + 1(\sigma/\sigma_m)^2]$, where v_{sc} is the SAW velocity for the conductive 2DES and v_{oc} is the velocity for a depleted electron system. Experimentally, we find, in the nonlinear regime, that the total change of the SAW velocity remains constant, in spite of the large intensity I_{SAW}. The curves are only shifted towards larger conductivity σ (Fig. 3). In order to understand this behavior, one has to consider the limiting cases for the conductivity: For zero gate bias, the electron density is too large to be bunched into stripes, therefore the SAW velocity is the same as for small SAW intensity. For a fully depleted electron system, the SAW velocity reaches its maximum and is obviously independent of the SAW intensity.

In summary, we have investigated the interaction between a low-dimensional electron system in a semiconductor quantum well and a surface acoustic wave of very large amplitude. The acoustoelectric interaction is now governed by strongly nonlinear effects, leading to a bunching of charge in the potential wells of the SAW. In a first experiment, we were able to directly observe the phonon drag of the carriers in the transition between the weak momentum transfer and a fully trapped regime. In a second experiment, we find that the electronic SAW attenuation strongly decreases with increasing SAW amplitude. Both experiments can be described as employing a nonlinear theory of acoustoelectric interaction in 2D systems.

We thank J. P. Kotthaus and S. Böhm for many enlightening discussions, and D. Bernklau and H. Riechert for the growth of the excellent MBE structures. We gratefully acknowledge the technical assistance of S. Manus and the generous financial support by the Siemens AG and the German Israeli Foundation.

[1] M. P. Lilly, J. P. Eisenstein, L. N. Pfeiffer, and K. W. West, Phys. Rev. Lett. **80**, 1714 (1998).
[2] A. D. Wieck, H. Sigg, and K. Ploog, Phys. Rev. Lett. **64**, 463 (1990).
[3] K. Nagamune, T. Noda, H. Watabe, Y. Ohno, H. Sakaki, and Y. Arakawa, Jpn. J. Appl. Phys. **35**, 1151 (1996).
[4] M. J. Hoskins, H. Morko, and B. J. Hunsinger, Appl. Phys. Lett. **41**, 332 (1982); W. J. Tanski, S. W. Merritt, R. N. Sacks, D. E. Cullen, E. J. Branciforte, R. D. Caroll, and T. C. Eschrich, Appl. Phys. Lett. **52**, 18 (1988).
[5] C. Rocke, S. Zimmermann, A. Wixforth, J. P. Kotthaus, G. Bohm, and G. Weimann, Phys. Rev. Lett. **78**, 4099 (1997).
[6] V. I. Talyanskii, J. M. Shilton, M. Pepper, C. G. Smith, C. J. B. Ford, E. H. Linfield, D. A. Ritchie, and G. A. C. Jones, Phys. Rev. B **56**, 15 180 (1997).
[7] A. Wixforth, J. Scriba, M. Wassermeier, J. P. Kotthaus, G. Weimann, and W. Schlapp, Phys. Rev. B **40**, 7874 (1989).
[8] R. L. Willett, M. A. Paalanen, R. R. Ruel, K. W. West, L. N. Pfeiffer, and D. J. Bishop, Phys. Rev. Lett. **65**, 112 (1990).
[9] R. L. Willett, R. R. Ruel, K. W. West, and L. N. Pfeiffer, Phys. Rev. Lett. **71**, 3846 (1993).
[10] J. M. Shilton, D. R. Mace, V. I. Talyanskii, M. Pepper, M. Y. Simmons, A. C. Churchill, and D. A. Ritchie, Phys. Rev. B **51**, 14 770 (1995).
[11] M. Rotter, C. Rocke, S. Böhm, A. Lorke, A. Wixforth, W. Ruile, and L. Korte, Appl. Phys. Lett. **70**, 2097 (1997).
[12] E. Yablonovich, D. M. Hwang, T. J. Gmitter, L. T. Florez, and J. P. Harbison, Appl. Phys. Lett. **56**, 2419 (1990).
[13] In 3D systems a nonlinear theory of acoustoelectric interactions was developed in a number of papers; see, e.g., P. N. Butcher and N. R. Ogg, Brit. J. Appl. Phys. (J. Phys. D), Ser. 2, **1**, 1271 (1968); P. K. Tien, Phys. Rev. **171**, 970 (1968).
[14] K. A. Ingebrigtsen, J. Appl. Phys. **41**, 454 (1970); M. V. Krasheninnikov and A. V. Chaplik, Sov. Phys. JETP **49**, 921 (1979); A. L. Efros and Y. M. Galperin, Phys. Rev. Lett. **64**, 1959 (1990).
[15] A. Y. Shik, Semicond. **29**, 697 (1995).
[16] A. O. Govorov, Phys. Rev. B **51**, 14 498 (1995).
[17] M. Rotter, A. Wixforth, W. Ruile, D. Bernklau, and H. Riechert, Appl. Phys. Lett. **73**, 2128 (1998).